PROCEEDINGS, 48th Workshop on Geothermal Reservoir Engineering
Stanford University, Stanford, California, February 6-8, 2023
SGP-TR-224

Fluorescein Tracer Testing on the 4100L – A Preliminary Examination of Initial Arrival in Wells and the Drift at the Second EGS Collab Testbed

Earl Mattson[1], Mitchell Plummer[2], Ghanashyam Neupane[2], Vince Vermeul[3], Dana Sirota[3], Mathew Ingraham[4], Tim Kneafsey[5] and the EGS Collab Team

hydro.mattson@gmail.com

[1]Mattson Hydrology LLC, Victor, Idaho, USA

[2]Idaho National Laboratories, Idaho Falls, Idaho, USA

[3]Pacific Northwest National Laboratory, Richland, Washington, USA

[4]Sandia National Laboratories, Albuquerque, New Mexico, USA

[5]Lawrence Berkeley National Laboratory, Berkeley, California, USA

Keywords: EGS, Collab, tracers, fracture transport, SURF

ABSTRACT

In the summer of 2022, four fluorescein injection tests were conducted in an attempt to characterize the fracture system and its flow evolution during the EGS Collab Project's 2.5-month-long hydraulic circulation test in the 4100-ft level drift of the Sanford Underground Research Facility. These tracer tests were conducted in a fractured network that was previously hydraulically stimulated in the Yates Amphibolite crystalline rock formation hosting the second EGS Collab testbed. Fluorescein was detected in numerous production wells above, below and within straddle packers as well as in the ceiling, wall, and floor of the adjacent drift. Outflow measurements from production wells by themselves are not sufficient to describe the fracture geometry between the injection and production wells. Results of the tracer tests provided the travel time from the injection well to the production well and leakage points along the drift. This additional information is used to develop conceptual model for flow paths and fracture system. In the EGS Collab second test bed, it appears there may be two major fracture sets that intersect the drift based on tracer arrival times to various production points. This paper describes the water flow pathways from an injection well through a hydraulically fractured rock to production wells and the drift, using flow rate discharge data and results of three tracer tests.

1. INTRODUCTION

The EGS Collab project is performing intensively monitored rock stimulation and flow tests at the 10-m scale at the Subsurface Underground Research Facility (SURF) to determine challenges in implementing enhanced geothermal systems (EGS). This project, supported by the U.S. Department of Energy, gathered data from two separate field tests in order to understand water flow in fracture rock and heat exchange processes between the rock and the injected water to build confidence in numerical modeling of these processes. Experiment 2 was designed to examine hydraulic shearing and fluid flow in a test bed at SURF located at a depth of about 1.25 km (the 4100-ft level) in amphibolite under a controlled set of stress and fracture conditions.

2. EXPERIMENT 2 BACKGROUND

The EGS Collab Experiment 2 testbed consists of 9 boreholes, and two earlier-drilled characterization boreholes. The initial plan was to have a central borehole (TC [central]) to be used for injection, and four open production wells (TL, TU, TN, TS, where "T" stands for "test", "L" for lower, "U" for upper, "N" for north, and "S" for south) surrounding the injection well (Figure 1). The production boreholes fan out to provide different distances between the wells depending on the depth from the collar. Since the wells were drilled before stimulation activities, it was expected that stimulated fractures would intersect at least one production well. In addition, there are two pairs of monitoring wells oriented approximately orthogonal to the injection well above and below the stimulation zone. The monitoring wells (DMU, DML, AMU, AML, where "D" stands for drift, "M" for monitoring, "A" for alcove) are oriented to span the stimulation/flow zone. The monitoring wells each contained a suite of geophysical monitoring equipment that were grouted in-place with a cement slurry.

The host rock for the 4100 level Experiment 2 test bed is the Yates Unit of the Poorman Formation, which is an amphibolite consisting of amphibole, plagioclase, and chlorite with minor amounts of sulfides. The rock underwent deformation during the Precambrian (Paleoproterozoic) and developed fractures that were subsequently healed with vein minerals consisting primarily of calcite and quartz (see Ulrich et al., 2022 for more details). Natural fractures were characterized from mapping fracture and weep zones in the drift, and fractures and veins in cores from the boreholes. Fracture orientations were determined from acoustic and optical televiewers.

With only a few exceptions, the fractures in the Experiment 2 test bed are healed and show little indication of being significantly transmissive. During drilling, there was no evidence of connected fractures based on circulation data. After completion of the boreholes, the boreholes were filled with water and the rate of water loss was measured. All boreholes lost water to the formation at low rates with the exception of borehole DMU (had a higher rate, Kneasfey et al., 2022a) and some initial outflows from borehole AML before it began losing water. The water loss data show the cumulative losses over the drilling period ranged from approximately 20 to 180 mL/day. Subsequent pressure-pulse results show that the rock has a uniformly low permeability with total-borehole values ranging from 6.9×10^{-19} to 4.6×10^{-18} m^2 for the majority of the tests (Kneafsey et al., 2022a).

The central well, TC (green line in Figure 1), had three stimulations conducted in mid-March 2022 including a ramped flow, a high flow rate, and oscillating pressure (Kneafsey et al., 2022b). The shallowest stimulation occurred between the 145.0-152.9-ft interval. This was a high-rate stimulation (5 L/min, 400 L of water) with water breakthrough into TN (149.8-ft as indicated by jetting water), TL, and at the corner of Site A and the main drift. The middle stimulation was conducted in the TC 168.7-176.6 ft interval and was a cyclic stimulation with only 40 liters of water injected. Effluent was observed from TN, TL, and TS. The stimulation did not seem to intersect TU. The deepest TC stimulation (192.4-200.3 ft), was started with an injection rate of 3 L/min until breakdown the rock, then the injection rate was reduced to a very low rate (up to 400 mL/min [~300 L total]) for the remainder of the stimulation. Borehole TN received most of the injected water from the TC stimulations and the distributed temperature system (DTS) in AMU suggested breakthrough in this monitoring well with a small amount of water produced at the AMU well head (see Kneafsey, 2023 for more details).

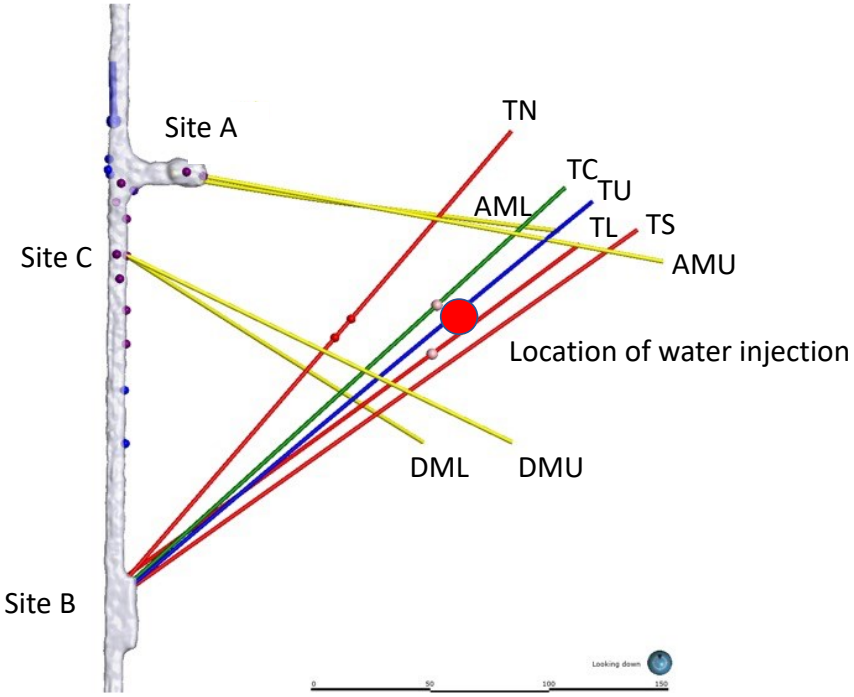

Figure 1. Plan view of Experiment 2 well layout and location of the water injection point for the long-term injection test.

Two 5 L/min short-term injections were conducted in early-May in TC. The shallow stimulation intersected DML whereas the TC middle stimulation intersected DML as well as the drift ceiling near the alcove/drift intersection. From the stimulation short-term injection test results, the best fracture connection was determined to be from TC to TU. However, since the TU fracture intersection was further from the drift, it was decided to make TU the injection point for the long-term flow test to minimize potential flow intersection with the drift (blue line Figure 1). A continuous flow was started on May 19 at 2 L/min. This injection rate was maintained for approximately 10 days when it was decided that the recovered rate from the production wells was not large enough to develop a thermal breakthrough. The injection rate was increased to 3.0 L/min on May 24 and subsequently increased to 3.4 L/min on May 26. With the exception of a two pump/power issues (see Table 1), 3.4 L/min injection rate was maintained in TU for the remainder of the test.

Table 1 Long-term TU injection test information

Date	Flow Rate	Notes
5/19/22	2 L/min	Weeps in drift
5/24/22	Increased from 2 to 3 L/min in 0.25 L/min increments	TN interval recovery more than doubled increasing from 223 to 505 mL/min. TC interval had a slight increase from 101 to 113 mL/min. Overall recovery increased from 31% to ~39%. Walls of the drift seem to become more wet.
5/26/22	Increased injection rate from 3 to 3.4 L/min in 0.2 L/min increments.	TN interval recovery increased from 550 to ~630 mL/min (14.5%) TC had a slight increase from 119 to 133 mL/min (11.7%).
6/4/22 to 6/15/22	Flow stopped pump failure	Approximately 10 days without injection while pump was being repaired
7/18/22	Brief injection interruption	Power outage for a few hours
8/17/22	Injection stopped	Production wells were shut-in, water production in the drift decreased.

3. WATER FLOW

Measurements of the production well discharge over the 2.5-month constant rate injection suggest that the major injected water flow pathway shifted towards the alcove/drift intersection over time. Drift measurements from the from the drift ceiling and walls suggest a dynamic flow of water in secondary flowing fractures from the northern part of the drift towards the south. It also appears that disruptions in the continuous injection of water had a relatively larger effect on these secondary discharges as compared to the higher flowing production wells. Analysis of the water flow rates from the two drift sumps suggest that most of the injected water bypassed the production wells and was discharged to the base of the drift near the alcove/drift intersection.

3.1 Production Wells

A straddle packer was placed in each production well to isolate flow into each production well into three separate zones; the collar (the drift to the upper packer), the interval (the zone between the upper and lower packer) and the bottom (from the bottom of the lower packer to the tip of the borehole). Since the packer straddle interval could most precisely isolate a flowing fracture, it was typically positioned over the highest flowing fracture.

Figure 2 depicts the flow rate from production wells TS, TC and TN for the three isolated zones in the wells. TL exhibited very little discharge. The injection into TU was fairly continuous with the exception of a ten-day hiatus near the beginning of the long-term flow test and a brief shutdown in July due to a power issue. Flow rates in TS decreased from 200 mL/min at the beginning of the test to near zero in early July (Figure 2A). This decrease is generally correlated with a similar decrease in the TN interval flow and an increasing TN collar flow and continued throughout July. On July 28, the TN packer interval was moved 10.5 feet closer to the drift to capture this high flow pathway (as noted by the last three orange data points in Figure 2C)

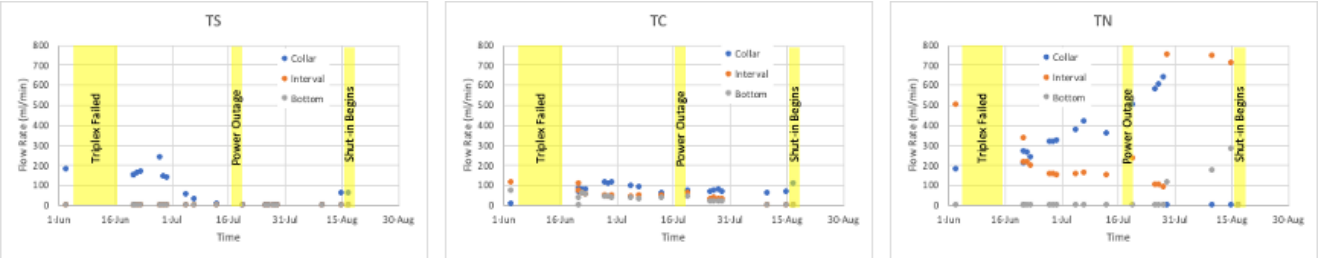

A) **B)** **C)**

Figure 2: Production wells flow rates as a function of time for A) production well TS, B) production well TC, and C) production well TN.

3.2 Drift Measurements

Water flux measurements were manually measured from various drips from the ceiling, wall weeps, and grouted monitoring wells. In general, ceiling drips appear to be in groups of multiple dripping points within ~10 square feet and were subsequently collected by hanging tarps from the ceiling to a common collection point. Wall weeps were collected using tissue paper as a wick to produce a localized dripping point. Monitoring well samples were collected at leaking conduit seals. Although we were able to collect the water sample in the drift, the location and flow pathway through the grouted well has some uncertainty. Other wall weeps/ceiling drips existed in addition to those shown in Figure 3 (A-C), but these were generally at such low flow rates that measurement was difficult.

In general, the flow rates were fairly steady, however there was a shift of water fluxes from the Site A, AMU, the Corner tarp, and Site C (all at the northern extend of the test site) to the south (Sites 6, 7 and 7.5) in late June and July. The Site C tarp, (a ceiling tarp adjacent to the DMU/DML monitoring well collars) was the highest flowing ceiling/wall weep with a flow rate of ~60 mL/min (Figure 3A). This flow steadily decreased to approximately 30 ml/min throughout July, then remained steady to the end of the injection test. At the Site A, drips from ceiling, AMU, and the corner tarp also exhibited a slight decrease in flows. In late June, new water flow drips in the drift ceiling appeared south of Site C (Figure 3B) along with a spike of water in DMU in late July after a brief power outage.

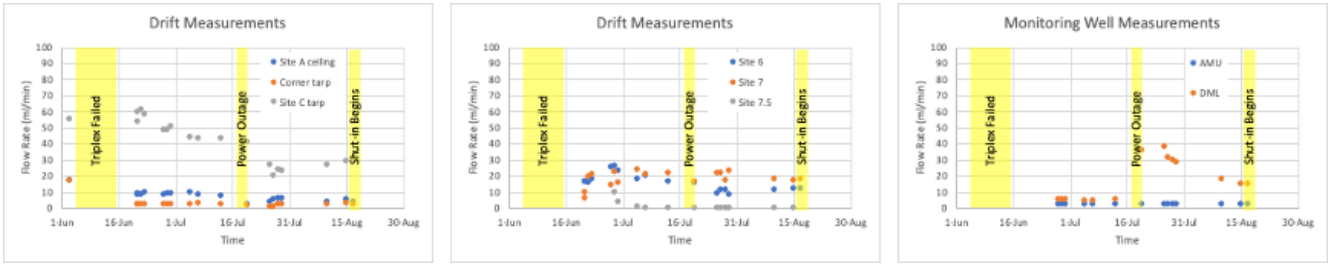

A) **B)** **C)**

Figure 3: Drift ceiling drips and monitoring wells flow rates as a function of time.

Disruption in the injection may change flow pathway dynamics further from the injection point. As seen in Figure 3, the triplex failure in early June and the brief power outage may be correlated with changing discharge rates in these secondary discharge locations. Figure 3A illustrates a discharge rate drop from ~20 ml/min before the triplex failure to ~4 ml/min after injection was reestablished. The initiation of water dripping in the southern part of the drift (Figure 3B) also started near this time. Flow from the grouted monitoring well DML substantially increased after a brief power outage in July (Figure 3C). Changes in the production well closer to the injection point did not exhibit a similar effect, albeit the discharge rate was much higher than those in the drift ceil/wall weeps.

3.3 Water Balance

Prior to termination the TU injection, the water discharge rate from sumps in the main drift and the production wells were measured and compared to the TU injection rate. As the steady state injection into TU continued, a free water surface developed along the main drift, south of Site A. In some locations, the water surface was above the drift floor gravel surface whereas other places a hole was dug in the drift ballast to find the water surface. A laser level was used to mapping the free water surface elevation along the drift revealing that the water formed a mound just south of the Site A intersection (Figure 4). Water flowed to the north to a ditch in the ballast and the water level in this ditch was controlled by a sump pump with a mechanical float. The water that flowed to the south also terminated in a sump constructed in Site B. The Site B sump also was the disposal of any water produced in the production wells.

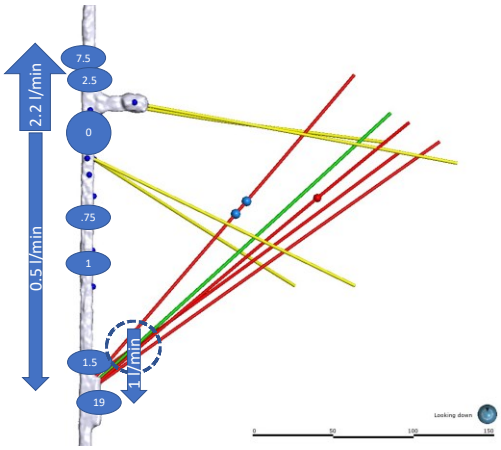

Figure 4: Free water surface elevation (in inches) below the laser level datum along the main drift, flow direction determined by gradient, and rates determined from the sump pump discharges.

Total water recovery from the production wells, ceiling and wall weeps, and flow through the floor was estimated from two sump discharge rates. The northern ditch produced 2.2 L/min whereas the southern sump produced 1.5 L/min for a total of 3.7 L/min. This value is slightly higher (< 10%) than the TU injection rate of 3.4 L/min. This slight overestimate may be due to manual operation of the North ditch pump which would have released some water stored in the drift ballast. Figure 5 illustrates the location of the surface water divide and the calculated water fluxes through the ballast of the main drift and the water recovery from the production wells. The production wells capture approximately 30% of the flow whereas the drift (ceiling drips, wall weeps, and water egress through the drift floor into the ballast) accounted for the remaining ~70%. Based on measurements of the major ceiling drips and wall weeps (~3%), most of the water entered the drift ballast through the drift floor (~67%). The water flux (~2.5 L/min) coming through the drift floor was the termination point of the major flow pathway from the TU injection well. Based on the location of the surface water mound and tracer detection in the water accumulated over ballast, this fracture enters the drift floor just south of the Site A alcove intersection with the main 4100 drift (~20 feet south of the midline of Site A alcove).

4. TRACER TESTING

Four fluorescein tracer tests were performed during the long-term circulation test (Table 2). All tests used the same injection point in TU located at 177.9 ft. Tracer was detected at numerous points in the production wells, in two of the grouted monitoring wells, and at ceiling drips, wall weeps, and the floor of the drift. Complete tracer breakthrough curves are only available for a limited number of tracer detection points due to a limited number of fraction collectors and accessibility to the 4100 level during these tests.

Table 2: Fluorescein pulse injection tests and detection locations.

	Fluorescein Detection Location							
Injection Date	TNI	TCI	TCB	Site C Tarp	DML	AC Wall	TNC	Limited data for:
06/01/22	BTC	BTC	BTC	BTC	x		x	AMU, Site A ceiling, Corner Tarp
06/22/22	BTC	BTC*		BTC			x	
07/26/22	BTC	BTC*	x		x	x	BTC	A-C puddle
07/29/22**	BTC			BTC*	BTC*	BTC*		TNB, A-C puddle

Notes:
* partial BTC (missing beginning, middle or end data)
x tracer detection
** New packer location for TNI and TNB (10.5 feet closer to drift in higher flow zone)

To conduct a tracer test, approximately 300 ml of a concentrated tracer cocktail (10,000 mg/L) was placed in one of the Quizix pump cylinders by activating a pump inlet 3-way valve. The stock tracer solution consisted of four grams of reagent grade fluorescein mixed with 400 mL of nano-pure (NP) water in a bottle. The second cylinder was filled with the service water from the 4100 pressurized water supply line. Both cylinders were then pressurized to match the injection pressure. The tracer cocktail was injected at 50 mL/min into the main injection hose through 25 feet of 5.9 mm ID SpirStar hose (blue line in Figure 5). At this point, the tracer cocktail mixed with the 3400 mL/min injection water and was transported to the injection well packer interval (orange line in Figure 5). Then tracer was transported through the rock fractures to a production well (yellow line in Figure 5), a monitoring well, or the drift. For the production wells, tracer was returned to the main drift instrument panel via 295 ft 12.8 mm ID SpirStar hose at the production well effluent flow rate (purple in Figure 5). Water samples were either manually collected and immediately analyzed or collected in a fraction collector overnight and analyzed the next morning.

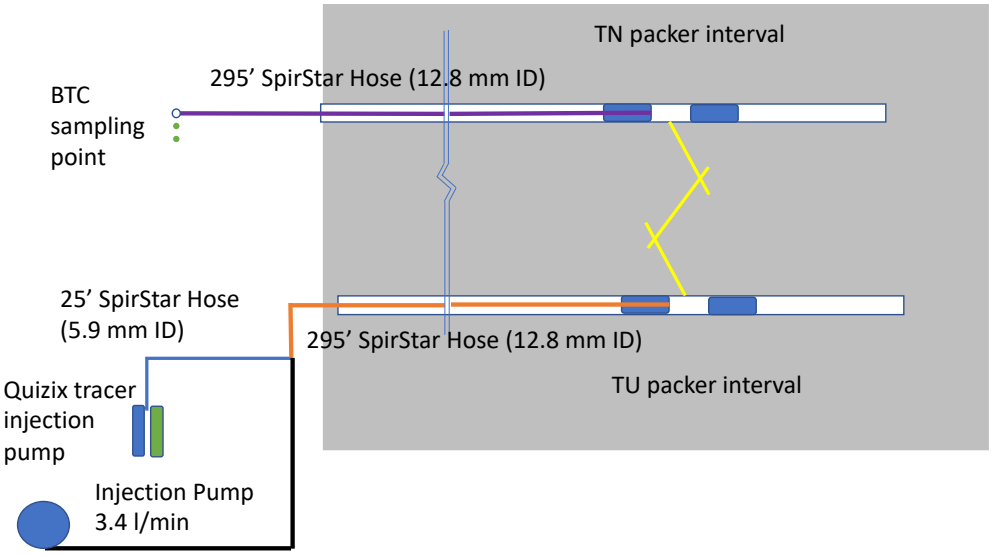

Figure 5: Tracer injection system for cross-well tracer testing.

Both the leftover mass of fluorescein in the stock solution and trapped mass of fluorescein in the Quizix pump and flow line were retrieved to obtain the exact mass of fluorescein injected into the testbed. The trapped mass of fluorescein in the Quizix pump assembly and flow lines were obtained by backflowing and rinsing the Quizix pump cylinders, valves and flow lines.

All samples were analyzed at the test site for fluorescein using an Ocean Optic spectrophotometer system (Ocean optic FIA-SMA-FL-UTL cell, PX-2 pulsed xenon lamp, QEPRO spectrophotometer). For analysis of fluorescein, a beam of excitation radiation at 484.22 nm wavelength was used. The mean wavelength of emission band was at 518 nm. For each sample, three scans average fluorescence count was recorded with 5 sec as integration time for each scan. Background fluorescence values were established using the pre-tracer injection production water from each major producers and corrected either during analysis (for TN-interval samples) or subsequently during data processing (for other producers). Prior to each analysis, a series of fluorescein calibration standard solutions were prepared using the TN-interval background water for construction of calibration curve with $R^2 > 0.99$. Consequently, the recorded fluorescence count of each sample was converted to fluorescein concentration using the relationship between fluorescence counts and fluorescein concentration in the standards.

4.1 Analysis of the tracer breakthrough curves

Tracer tests conducted at various times and collected at different locations (Table 2) were used to test if measurable differences in velocity and dispersion could be detected over the two-month circulation test. In addition to the tests listed in Table 2, two equipment tracer tests were conducted with fluorescein or sodium chloride. Other tracer tests include, the injection of two rhodamine B sorbing tracers, a NaCl injection which the BTC was monitored by the inline electrical conductivity probes, and an 8-hour duration NaCl injection for electrical resistivity tomography analysis. Finally, the water injection system was configured such that the local mine water (~400 uS/cm) and mine water treated by reverse osmosis (~10 to 100 uS/cm) could be automatically switched to create a series of varying electrical conductivity pulses throughout the long-term constant injection. For this paper, only the fluorescein tests will be discussed.

To determine the velocity and dispersion of the tracer in the fracture segment from the tracer breakthrough curves, the tracer concentration input function at the packer interval in the TU injection well and the tracer breakthrough curve at the tracer discharge location must be known. The tracer injection/recovery system can be divided into four segments: 1) the tracer pump and initial injection hose, 2) a larger diameter main injection hose, 3) the rock fracture system, and 4) the return hose from the packer interval and bottom segments. These four segments are schematically represented in Figure 5 as the blue line, orange line, yellow line, and the purple line respectively. For production wells, the tracer discharge location would be the packer interval. For ceiling drips and wall weeps in the drift, there is no segment 4. Uncertainty in the location of fracture intersections with monitoring wells and production wells above and below the production well packers made velocity and dispersion calculations uncertain for these locations.

Two injection equipment tracer tests were conducted to assess the amount of dispersion created by the Quizix injection pump and in the SpirStar injection hoses. These results indicated that there was significant dispersion of the tracer as it traveled from the injection pump to the TU injection interval in the borehole (Figure 6). The fluorescein tracer test was conducted using the TL packer interval. TL interval had zero discharge making it an ideal equipment injection/discharge test. To measure discharge from the TL interval, 3.4 mm diameter SpirStar tubing that terminated at Site B in the drift was used. Tracer concentration as a function of time was measured. Figure 6 illustrates the calculated concentration results assuming plug flow occurs through the hoses and tubing (blue line) compared with the measured tracer concentrations. As shown in this figure, the measured tracer concentrations are about $1/10^{th}$ of the value of the expected peak concentrations, which indicate the presence of Gaussion dispersion in the SpirStar hoses.

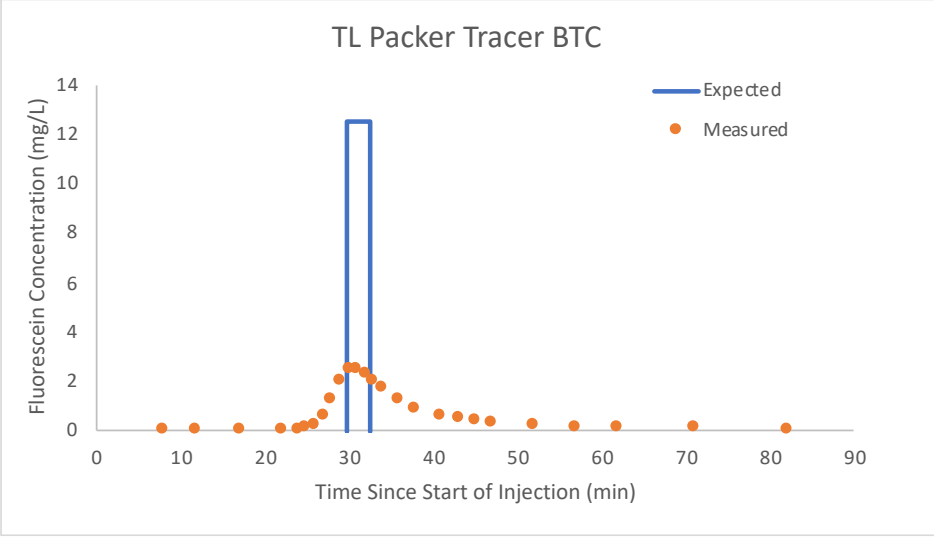

Figure 6: Expected and measured breakthrough curves at the packer interval

As part of this analysis, we sought to remove the effect of dispersion in the SpirStar hoses that carried fluid to and from the fracture system. To estimate dispersion in the hoses, the modeled tracer breakthrough curves were fitted to the two tracer tests aimed at measuring transport behavior in the hoses. Tests examined transport in the (1) 25-ft long hose that brings tracer to the primary fluid delivery hose (Figure 7A) and (2) the combination of hoses delivering and recovering injected fluids (Figure 7B). Both tests were conducted at fluid flow rates considerably less than that used in the actual tracer tests. Fitting these data via adjustment of velocity and dispersion indicated that the dispersion was considerably less than expected based on steady-state Taylor dispersion theory. Therefore, an attempt to fit the data to a model that used mathematical relationships describing pre-asymptotic Taylor dispersion (Taghizadeh et al. 2020). However, a simple dispersivity model (dispersivity = 0.9 m) provided a better estimate of the dependence of dispersion on velocity (7), and the latter relationship was used to predict the effect of dispersion in the tubing in subsequent analyses, which were conducted at significantly higher fluid injection rates.

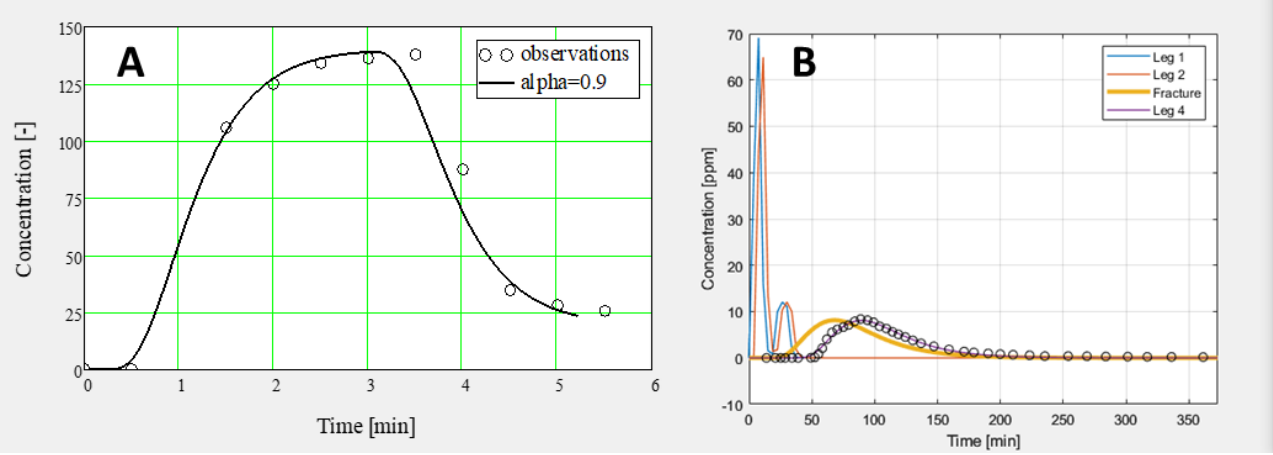

Figure 7. (A) Fluorescein tracer breakthrough curve (open circles) from flow through the 25-ft of tracer delivery tubing. Solid line illustrates model fit using a dispersivity of 0.9 m. (B) Breakthrough curves (open circles) from return flow of tracer injected into, and collected from, the TNI June 1st injection by fitting the velocity, dispersion and mass fraction of the segment 3 fracture. Different segments (see color segment scheme in Figure 5) refer to the sequence of hoses and tubing, for which exit concentration is calculated. Solid line illustrates model fit of the fracture using a dispersivity of 0.9 m for the other three segments.

To estimate velocity and dispersion from each of these curves, the tracer transport process was simulated using MATLAB-based solutions of the transport equations with a four-step injection input and a 1-D domain that accounted for the calculated velocity and estimated dispersion in each of the sections of tubing carrying fluid and tracer to the fracture zone. Fitted velocities, dispersion coefficients and calculated dispersivities for the fracture segment are provided in Table 3.

Table 3. Model fitted velocity, dispersion, and mass balance results for the fracture segment for the first three fluorescein tracer tests.

Date	Location	Qwell	M	V	D	Dispersivity
		ml/min	-	m/s	m^2/s	m
6/1/22	TNI	540	0.6908	0.0031	0.0059	2
6/22/22	TNI	195	0.7218	0.0007	0.0052	7
7/26/22	TNI	101	0.5541	0.0004	0.0068	17
6/1/22	TCI	120	0.6379	0.0009	0.0030	3
6/22/22	TCI	56	0.8382	0.0002	0.0010	5
6/1/22	Tarp	55	0.3220	0.0021	0.0016	1
6/22/22	Tarp	61	0.4720	0.0066	0.0145	2
7/29/22	Tarp	27	0.2695	0.0022	0.0041	2

4.3 Fluorescein Test Interpretations

Using water discharge measurements in the production wells and the drift ceiling/wall weeps, calculated water mass balance, and the first detection of tracer arrival during tracer tests, a conceptual model for water flow in the fractures was developed. This conceptual model was then used to interpret the role of production water discharge and its utility on predicting the water velocity in a fracture rock system.

4.3.1 Water and tracer conceptual model

During Collab's 2.5-month flow test, water discharge varied from the production wells as a function of time suggesting a change in the flow dynamics within fractures at the 10-meter scale (section 3.1). In addition, these flow changes were also seen at the 50-meter scale (i.e., in the drift) as evident of flow rate changes in ceiling and wall weeps (section 3.2). Variability in the discharge in both the production wells and the drift occurred despite attempts to maintain a constant injection rate.

The water mass balance calculations (section 3.3) suggest that there is major flowing fracture(s) from the TU injection location to the area at the alcove/drift intersection. This conceptual model is supported by the time of first detection of fluorescein tracer in the production wells and the drift. Figure 8a illustrates the spatial distribution of the time of first tracer detection (blue dots with time in hours) for the July 26-29 tracer tests. As seen in this figure, tracer is first detected in the two production wells (TCI 0.3 hrs, TNI 0.4 hrs) suggesting a fast flow pathway velocity of 34 and 40 m/hr for TCI and TNI respectively. The fastest tracer detection velocity was located at the floor seep at the alcove/drift intersection (46 m/hr) despite being about 3 times further away from the TU injection point as than the production wells. Other tracer detections in the drift (the Site C tarp and the Site A ceiling drip) took at least twice as long (i.e., ½ the velocity) compared to the alcove/drift detections even though the distance of all three tracer discharge points from TUI are approximately the same.

The early detection of tracer at the alcove/drift floor is collaborated by the water mass balance analysis and suggests a major flow pathway has been developed from TUI to the drift/alcove intersection location and is represented by the large red arrow in Figure 8A. This flow path appears to pass through/near the two production wells, TCI and TN. The Site A and C detections suggest that there are secondary flow pathways that are either branching off from the main fracture near these detection locations, or the detections possibly represent long secondary flow pathways.

Although the water measurements and the tracer tests provide indications of the locations of travel pathways, the measurements do not provide quantitative information on the exact pathway the water and tracer travel through the fracture rock. Figure 8b includes a preliminary tomographic representation of the change in electrical conductivity of the July 26 sodium chloride tracer injection (Tim Johnson, PNNL, personal communication, 2023). An 8-hour injection of concentrated sodium chloride was followed by a purge of 400 uS/cm mine water. A tomographic image was developed 16 hours after injection (Figure 8B). As shown in this figure, there are a number of residual high concentrations of electrical conductivity that may represent the flow pathways of the concentrated salt water injection. The flow conceptual model shown in Figure 8a is consistent with the electrical resistive tomography (ERT) results. The ERT images can help to redefine the conceptual flow model for subsequent numerical analysis.

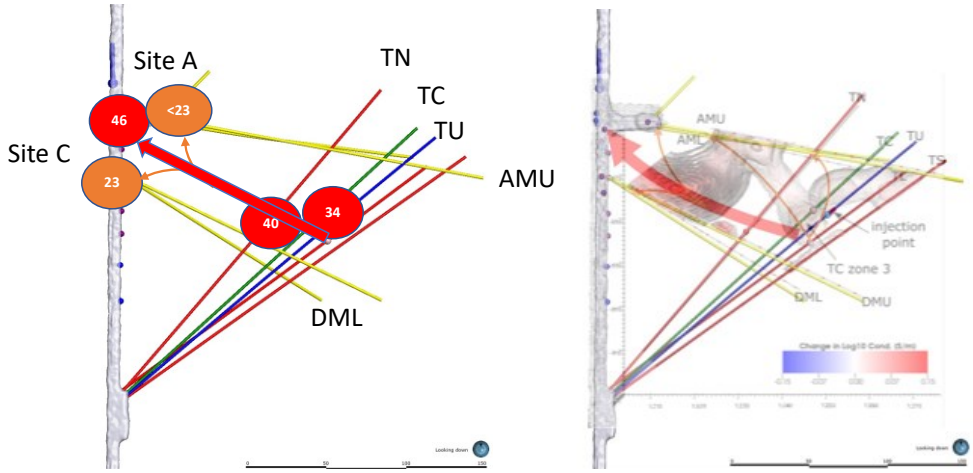

A) B)

Figure 8. A) Calculated tracer velocity of first detection of the July 26 – 29, 2023 fluorescein tracer test (in hours after injection) in the production wells and in the drift, B) conceptual model of tracer pathways from the injection well to discharge locations overlain with an electrical resistivity tomographic image from a salt water tracer injection on July 26.

4.3.2 Water discharge rate vs fracture velocity

The simplest conceptual model of water movement in a fracture from an injection well to a production well is a stream tube that connects the two points. In such a model, there would be numerous stream tubes from the injection location to the multiple discharge locations. In this case, the production well flow rate is considered to be the correct variable related to the tracer velocity in the stream tube. A second conceptual model of water flowing in a fracture could be described as a major flow pathway with points along the flow path where the water leaks into individual fractures. Although a major fracture flow pathway could also be considered a stream tube, in this case the velocity in the main fracture is not controlled by individual discharge flows. Depending on the tracer residence time in the main fracture compared to the tracer residence time in the secondary fracture, the production well discharge rate may have a small influence on the calculated velocity of the tracer between the injection and production locations.

Figure 9 illustrates the calculated fluorescein fracture velocity from tracer tests conducted on June 1, 22 and July 26, 2023 for TNI, TCI and the Site C tarp plotted against the well discharge rate. Results from this limited data set support the first conceptual model (simple flow through a stream tube) because the production well flow rates appear to be linearly related to the average tracer velocity to each discharge point. According to the water mass balance analyses, the majority of fracture flow is being discharged to the base of the drift near the alcove/main drift intersection. Despite the fact that both the drift and the TNI and TCI production wells intervals are approximately atmospheric pressure and the production wells? are located approximately 1/3rd the distance from the injection well as compared to the discharge locations in the drift, these wells only captured about 25% of the injected water. Schwering et al. (2023) examined the pressure response of the production wells during shut-in tests conducted at the end of the long-term flow experiment. The producing zones of these wells quickly reached a near-steady-state shut-in pressure, which indicates the near-wellbore fracture aperture was maintained while the injection at TU continued. After the TU injection was terminated, the producing zones slowly lost pressure which suggests closure of these near-wellbore fractures and no significant shear residual permeability (e.g., from shearing). This production well skin effect could explain the low production well recovery of the injected water.

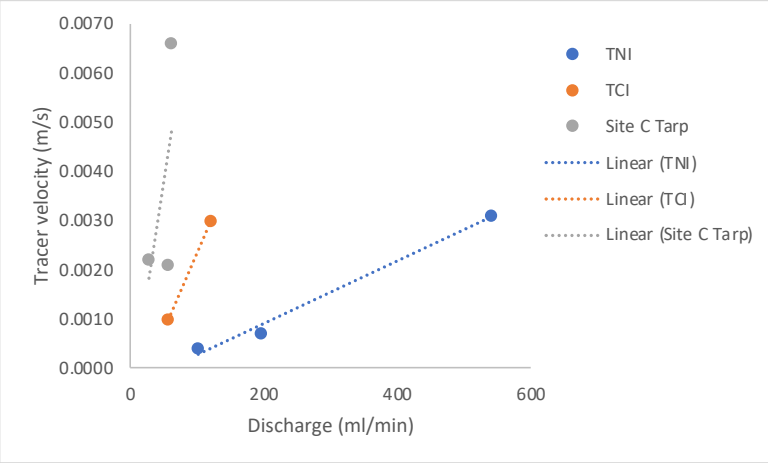

Figure 9. Relationship tracer velocity in the fracture and production wells TNI and TCI water discharge rates.

5. SUMMARY

Flow measurements as a function of time and location have been summarized for the Collab Experiment 2 long term constant rate injection test. These data suggest a dynamic flow regime within the test bed that becomes biased towards the drift tunnel over the 2.5-month injection test. Secondary fractures to ceiling drips/wall weeps appear to exhibit some level of dynamic behavior as seen in the changing discharge rate vs time and weep locations. Interruption of the injection rate seems to have a greater effect on the drift discharge rate changes as compared to the discharge rates seen in the production wells. It is unclear if this observation is related to the lower discharge rates in the drift discharges as compared to the production wells, or perhaps due to pore pressure dynamics.

A new numerical model was developed to account for tracer dispersion in the injection and extraction hoses, such that the fracture velocity and dispersion could be calculated more accurately. Modeling the tracer injection system results suggest that dispersion in hoses can be important. In this case, dispersion was larger in the hoses than that calculated in the fracture. Ignoring injection/production hose dispersion over-predicted the fracture dispersion. Performing a measurement to determine the hose dispersion at a number of injection rates would have provided more accurate hose dispersion calculations.

A flow and transport conceptual model was developed for the long-term flow test for Experiment 2. Data supporting this model suggests that a fast-flowing fracture system accounts for approximately 70% of the injected water flow that terminates in the drift floor near the alcove/drift intersection. The two production wells (TNI and TCI) between the injection well and the drift accounted for about 25-30% of the injected water despite being three times closer to the injection well as compared to the drift discharge location. Evaluation of the production well flow rates and the calculated fracture velocities suggest that the production well flow rates are correlated to the calculated average fracture velocities determined by the tracer breakthrough curves.

Possible EGS field implications from the Collab Experiment 2 long-term flow test results.

- Fracture flow dynamics are seen at the 10 and 50-meter scale despite maintaining a constant injection rate. If similar flow dynamics occurs at an EGS site, this flow dynamics could benefit heat extraction by accessing more parts of the fracture system. We were not able to ascertain the phenomena that changed the flow pathways. Controlling this flow dynamics will be difficult in the field.
- Calculation of potential dispersion in a tracer injection/extraction system should be evaluated prior to conducting field tests. The Collab tracer tests exhibited significant tracer dispersion in the 300-foot injection and extraction hoses. Preliminary analyses suggest that fracturing at depths of 10,000 feet in EGS systems will also have significant Taylor dispersion in their injection and extraction systems as well.
- Production wells may not cage the growth of an EGS flow system where the injection pressure is greater than the minimum principal stress and the fractures are hydro-propped. The production wells at the Collab Experiment 2 site only captured 25 to 30% of the injected water, the remainder of the water discharged in the drift. A review of previous EGS data indicates that water loss was a major concern at these sites. Although EGS is attempting to avoid faults, natural fractures will also be discharge structures that can alter the flow pathways to undesirable locations. Shut-in test results suggest that there exists a near well low permeability zone near the productions wells. The use of proppants at the production wells could increase the production well discharge rates by reducing well skin effects.
- The major flow pathway of the Collab Experiment 2 site did not appear to be collocated with MEQ events. Most of the MEQ events were located above the Experiment 2 test bed. The major flow pathway discharged to the drift floor. MEQ events appear to be biased above the flow zone and should be evaluated prior to drilling a production well in a location solely based on MEQ cloud density.

ACKNOWLEDGEMENTS

This material was based upon work supported by the U.S. Department of Energy, Office of Energy Efficiency and Renewable Energy (EERE), Office of Technology Development, Geothermal Technologies Office, under Award Number DE-AC02-05CH11231 with LBNL and other awards to other national laboratories. The United States Government retains, and the publisher, by accepting the article for publication, acknowledges that the United States Government retains a non-exclusive, paid-up, irrevocable, world-wide license to publish or reproduce the published form of this manuscript, or allow others to do so, for United States Government purposes. This paper describes objective technical results and analysis. Any subjective views or opinions that might be expressed in the paper do not necessarily represent the views of the U.S. Department of Energy or the United States Government. The research supporting this work took place in whole or in part at the Sanford Underground Research Facility in Lead, South Dakota. The assistance of the Sanford Underground Research Facility and its personnel in providing physical access and general logistical and technical support is gratefully acknowledged. We also thank the crew from RESPEC, who supported water sampling and flow measurements from wells and within the drift. The earth model output for this paper was generated using Leapfrog Software, copyright Seequent Limited. Leapfrog and all other Seequent Limited product or service names are registered trademarks or trademarks of Seequent Limited.

REFERENCES

Ingraham, M., Schwering, M., Ulrich, C., Doe, T., Roggenthen, W.M., Reimers, C., and the EGS Collab team (2020) Analysis of hydraulic fracturing on the 4100 level at the Sanford Underground Research Facility. Proceedings, 54th US Rock Mechanics/Geomechanics Symposium, ARMA 20-1158, 6 p.

Kneafsey T, Blankenship D, Dobson P, Burghardt J, White M, Morris J, Johnson T, Ingraham M, Ulrich M, William Roggenthen5 , Thomas Doe6 , Megan Smith4 , Jonathan B. Ajo-Franklin7 , Lianjie Huang8 , Ghanashyam Neupane9 , Tatiana Pyatina10 , Paul C. Schwering2 , Chet Hopp1 , Veronica Rodriguez Tribaldos1 , Yves Guglielmi1 , Chris Strickland3 , Vince Vermuel3 , Pengcheng Fu 4 , Hunter A. Knox3 , and The EGS Collab Team: The EGS Collab – Initial Results from Experiment 2: Shear Stimulation at 1.25 km depth. ; Proceedings, 47th Workshop on Geothermal Reservoir Engineering Stanford University, Stanford, CA (2022)

Kneafsey, T. J., Dobson, P. F., Ulrich, C., Hopp, C., Rodríguez-Tribaldos, V., Guglielmi, Y., Blankenship, D., Schwering, P. C., M., I., Burghardt, J. A., White, M. D., Johnson, T. C., Strickland, C., Vermuel, V., Knox, H. A., Morris, J. P., Fu, P., Smith, M., Wu, H., Ajo-Franklin, J. B., Huang, L., Neupane, G., Horne, R., Roggenthen, W., Weers, J., Doe, T. W., & EGS Collab Team. (2022b). The EGS Collab Project – Stimulations at Two Depths. Paper presented at the 56th US Rock Mechanics/Geomechanics Symposium, Santa Fe, New Mexico, USA.

Kneafsey, T., Robertson, M., Blankenship, D., Dobson, P., Schwering, P.C., Burghardt, J., White, M., Morris, J.P., Fu, P., Johnson, T., & EGS Collab Team: The EGS Collab - Discoveries and Lessons from an Underground Experiment Series, Proceedings, 48th Workshop on Geothermal Reservoir Engineering, Stanford University, Stanford, CA (2023).

Schwering, P., Ingraham, M., Vermeul, V., Burghardt, J., Johnson, T., Strickland, C., White, M., Hopp, C., Rodríguez Tribaldos, V., Kneafsey, T., Artz, T., Mattson, E., Doe, T., and the EGS Collab Team: Shut-In Testing on the 4100L - Implications on the State of Stress, Fractures, and Wellbores in the Second EGS Collab Testbed, Proceedings, 48th Workshop on Geothermal Reservoir Engineering, Stanford University, Stanford, CA (2023).

Sudhakar, M.R., and Thyagaraj, T., Role of Direction of Salt Migration on the Swelling Behavior of Compacted Clays, Applied Clay Science, 38, (2007), 113-129

Taghizadeh, E., Valdés-Parada, F., & Wood, B. Preasymptotic Taylor dispersion: Evolution from the initial condition. Journal of Fluid Mechanics, 889, A5. doi:10.1017/jfm.2020.56 (2020)

Ulrich, C., Dobson, P., Kneafsey, K., Roggenthen, W., Uzunlar, N., Doe, T., Neupane, G., Artz, T., Dobler, K., Schwering, P., Smith, M., Burghardt, J., (2022). Characterizing rock fractures and physical properties for Experiment 2 of the EGS Collab Project, Sanford Underground Research Facility. In Proc. 56th US Rock Mechanics/Geomechanics Symposium, Santa Fe, NM. American Rock Mechanics Symposium